Article

Nonradical Zinc–Barbier Reaction for Diastereoselective Synthesis of Vicinal Amino Alcohols

Lise Keinicke, Peter Fristrup, Per-Ola Norrby, and Robert Madsen

J. Am. Chem. Soc., **2005**, 127 (45), 15756-15761• DOI: 10.1021/ja054706a • Publication Date (Web): 25 October 2005

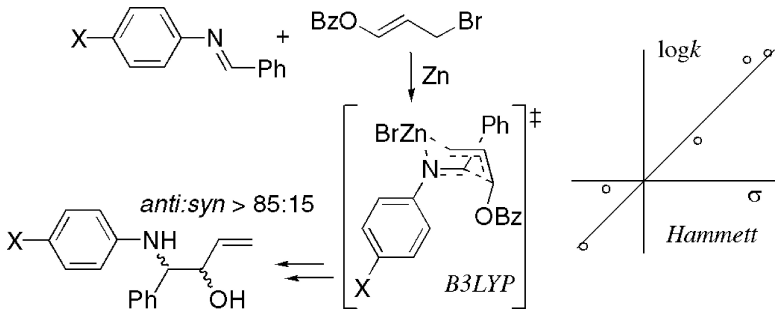

More About This Article

Additional resources and features associated with this article are available within the HTML version:

- Supporting Information
- Links to the 8 articles that cite this article, as of the time of this article download
- Access to high resolution figures
- Links to articles and content related to this article
- Copyright permission to reproduce figures and/or text from this article

View the Full Text HTML

J|A|C|S
ARTICLES
Published on Web 10/25/2005

Nonradical Zinc−Barbier Reaction for Diastereoselective Synthesis of Vicinal Amino Alcohols

Lise Keinicke, Peter Fristrup, Per-Ola Norrby,* and Robert Madsen*

Contribution from the Center for Sustainable and Green Chemistry, Department of Chemistry, Technical University of Denmark, Building 201, Kemitorvet, DK-2800 Lyngby, Denmark

Received July 14, 2005; E-mail: pon@kemi.dtu.dk; rm@kemi.dtu.dk

Abstract: A new protocol for the synthesis of vicinal amino alcohols is described. The method employs a Barbier-type reaction between an imine and 3-benzoyloxyallyl bromide in the presence of zinc metal. The addition products are debenzoylated to afford amino alcohols in good yields and with diastereomeric ratios greater than 85:15 in favor of the anti isomer. A Hammett study has been performed which strongly indicates that the allylation does not follow a radical mechanism, but instead an organometallic reagent is formed which subsequently reacts with the imine. A computational study based on this mechanism reproduces the observed diastereoselectivity with high accuracy, but only when a sufficiently large portion of the substrate is included.

Introduction

Vicinal amino alcohols are important structural elements in organic chemistry.[1] Many natural products, pharmacologically active compounds, and chiral auxiliaries contain amino alcohols as major recognition elements. Amino alcohols are also significant components in ligands for asymmetric catalysis.

Current strategies for stereoselective synthesis of amino alcohols are mainly based on olefin oxidation (Scheme 1), either through direct aminohydroxylation[2] or via other reactive functionalities such as epoxides[3] or aziridines.[4] These can be performed with good stereoselectivity but not always with complete regiocontrol. Alternatively, carbon nucleophiles can be added to protected α-hydroxyimines[5] or α-aminoaldehydes.[6] We have recently become interested in another strategy, where the amino alcohol is built in a convergent fashion by formation of the C−C bond. Recent applications of this approach include addition of dipolar reagents[7] or suitably functionalized organometallic reagents[8] to imines. Catalytic asymmetric Mannich-type reactions of α-hydroxyketones and imines using chiral ligands have also been reported.[9]

Under Barbier-type conditions using metals such as Zn and In, allyl bromides add to aldehydes and aldimines, yielding homoallylic alcohols and amines, respectively. It has recently been shown that acyloxyallyl bromides, derived from acyl bromides and acrolein,[10] can also be added to aldehydes to yield diols (Scheme 2, left).[11] Of particular interest to us was a recent report where in one case acetyloxyallyl bromide was found to add to a protected imine formed in situ from an α-amidosulfone, yielding an amino alcohol (Scheme 2, right).[8]

Scheme 1. Some Synthetic Strategies for Production of Vicinal Amino Alcohols

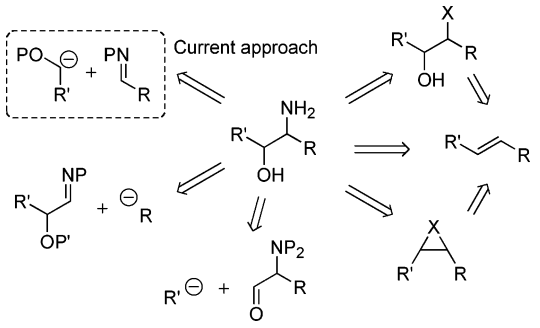

We have previously performed Barbier-type allylations of carbohydrate-based aldehydes, which combined with ring-closing metathesis forms a general route to cyclic polyols.[12] Amino alcohols could also be generated by allylation of hydroxyimines using allyl bromide in the presence of Zn, In, or Mg, which was used as a critical step in a recent synthesis of the calystegine alkaloids.[13] As an extension of this work, we

(1) Bergmeier, S. C. *Tetrahedron* **2000**, *56*, 2561−2576 and references therein.
(2) Li, G.; Chang, H.-T.; Sharpless, K. B. *Angew. Chem., Int. Ed. Engl.* **1996**, *35*, 451−454.
(3) (a) Larrow, J. F.; Schaus, S. E.; Jacobsen, E. N. *J. Am. Chem. Soc.* **1996**, *118*, 7420−7421. (b) Olofsson, B.; Somfai, P. *J. Org. Chem.* **2002**, *67*, 8574−8583.
(4) Hu, X. E. *Tetrahedron* **2004**, *60*, 2701−2743.
(5) Bloch, R. *Chem. Rev.* **1998**, *98*, 1407−1438.
(6) Reetz, M. T. *Chem. Rev.* **1999**, *99*, 1121−1162.
(7) Torssell, S.; Kienle, M.; Somfai, P. *Angew. Chem., Int. Ed.* **2005**, *44*, 3096−3099.
(8) Petrini, M.; Profeta, R.; Righi, P. *J. Org. Chem.* **2002**, *67*, 4530−4535.
(9) (a) List, B.; Pojarliev, P.; Biller, W. T.; Martin, H. J. *J. Am. Chem. Soc.* **2002**, *124*, 827−833. (b) Trost, B. M.; Terrell, L. R. *J. Am. Chem. Soc.* **2003**, *125*, 338−339. (c) Matsunaga, S.; Yoshida, T.; Morimoto, H.; Kumagai, N.; Shibasaki, M. *J. Am. Chem. Soc.* **2004**, *126*, 8777−8785. (d) Kobayashi, S.; Ueno, M.; Saito, S.; Mizuki, Y.; Ishitani, H.; Yamashita, Y. *Proc. Natl. Acad. Sci. U.S.A.* **2004**, *101*, 5476−5481.
(10) (a) Neuenschwander, M.; Bigler, P.; Christen, K.; Iseli, R.; Kyburz, R.; Mühle, H. *Helv. Chim. Acta* **1978**, *61*, 2047−2058. (b) Bigler, P.; Schönholzer, S.; Neuenschwander, M. *Helv. Chim. Acta* **1978**, *61*, 2059−2080.
(11) (a) Lombardo, M.; Girotti, R.; Morganti, S.; Trombini, C. *Chem. Commun.* **2001**, 2310−2311. (b) Lombardo, M.; Girotti, R.; Morganti, S.; Trombini, C. *Org. Lett.* **2001**, *3*, 2981−2983. (c) Lombardo, M.; Morganti, S.; Trombini, C. *J. Org. Chem.* **2003**, *68*, 997−1006.
(12) Hyldtoft, L.; Madsen, R. *J. Am. Chem. Soc.* **2000**, *122*, 8444−8452.
(13) Skaanderup, P. R.; Madsen, R. *J. Org. Chem.* **2003**, *68*, 2115−2122.

10.1021/ja054706a CCC: $30.25

Scheme 2. Barbier-type Synthesis of Amino Alcohols and Diols

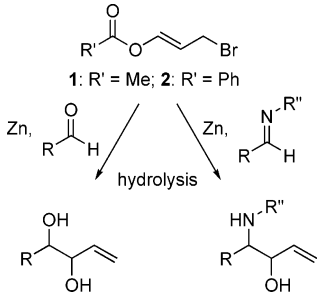

are currently investigating the scope of the C−C disconnection approach depicted in Scheme 1. In the current work, we present reactions of a model system and a mechanistic investigation of the title reaction, whereas synthetic applications will be reported separately.

As opposed to classical organometallic addition reactions such as Grignard, where an organometallic reagent is prepared and subsequently added to an electrophile, in allylation reactions run under Barbier conditions the metal is added to a solution already containing both the halide and the electrophile. Several mechanistic pathways have been suggested. The initial reaction could potentially be formation of a Grignard-type organometallic reagent, but the reaction is unusually tolerant and can even be performed in water, which would be expected to protonate the organometallic reagent rapidly.[14] Furthermore, formation of dimerization products, both of the allylic reagent and the electrophile, indicates a mechanism with single-electron transfer (SET) from the metal as the first step.[15] These observations make a SET mechanism plausible, but cannot exclude the more traditional mechanism via an initially formed, closed shell organometallic species. We therefore decided to study the mechanism of the title reaction in more detail.

Absolute rate measurements for the title reaction are complicated by the presence of a heterogeneous reagent, which precludes many types of spectroscopic monitoring and which may introduce mass transfer over phase boundaries as an important but unknown factor in the kinetic equations. We have elected to perform a Hammett study, which can be implemented as a competition experiment between the substrates and therefore is not sensitive to steps preceding the reaction with the electrophilic substrate. We have previously applied the Hammett methodology to a range of metal-assisted reactions.[16] As our current model system, we have chosen reactions with para-substituted *N*-benzylidene anilines. Benzoate reagent **2** was chosen over the corresponding acetate **1**, due to ease of handling and higher storage stability (Scheme 3).

Results and Discussion

Synthesis of Amino Alcohols 4. Imines **3a**−**f** were prepared from condensation of benzaldehyde and the corresponding anilines (see the Supporting Information for experimental details). The initial reactions and optimization experiments were

Scheme 3. Model System for the Allylation of Imines

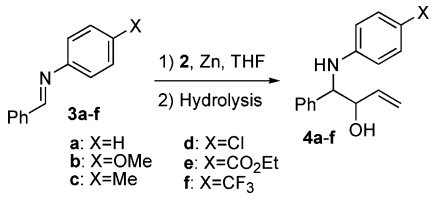

Scheme 4. Allylation of Benzylideneanilines **3a** and **3b**

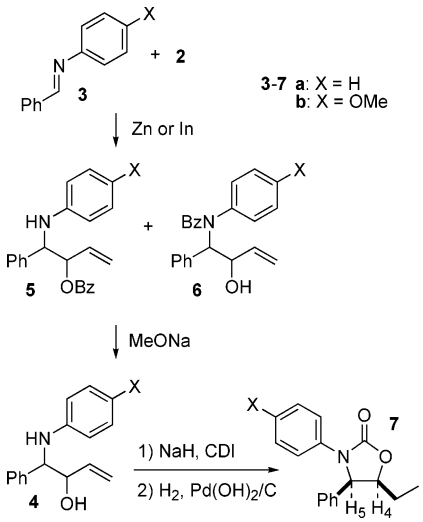

performed for the unsubstituted and *p*-methoxy-substituted substrates **3a** and **3b**, respectively. With the use of zinc in THF the desired allylation of the imine took place, but during the reaction the expected product **5a** was partially converted to the more stable amido alcohol **6a** by migration of the benzoyl group (Scheme 4). One major diastereomer of **6a** was observed. Heating the reaction mixture or changing the solvent to dioxane changed the ratio of **5a**/**6a**, but it was not possible to achieve high selectivity for one of the products. The highest isolated yields were 72% of **6a** using the initial reaction conditions and 50% of **5a** from the reaction in dioxane. However, the diastereoselectivity was high for both products. Subsequent debenzoylation gave **4a** in high overall yield, and with one diastereomer clearly dominating (90:10), showing that the major isomer was the same for both **5a** and **6a**. The major diastereomer could be assigned as anti by conversion of **4a** into oxazolidinone **7a** through treatment with 1,1-carbonyldiimidazole (CDI) followed by hydrogenation of the double bond. The final reduction was performed in order to avoid overlap of signals in the ^{1}H NMR spectrum. Comparison to literature data for the coupling constant $J_{4,5}$ in analogous compounds[17] verified the stereochemical assignment. Imine **3b** was subjected to the same reaction sequence as **3a** (Scheme 4), and the coupling constant $J_{4,5}$ in oxazolidinone **7b** indicated that the stereochemistry for this compound was also anti. The anti/syn ratio of **4b** was found to be 95:5, even higher than that for **4a**.

We have previously observed interesting changes in the selectivity of the Barbier allylation when changing the metal from Zn to In.[12,13] In the current case, imine **3a** was also allylated with **2** and indium metal in anhydrous ethanol (Scheme

(14) (a) Pétrier, C.; Luche, J.-L. *J. Org. Chem.* **1985**, *50*, 910−912. (b) Wilson, S. R.; Guazzaroni, M. E. *J. Org. Chem.* **1989**, *54*, 3087−3091.
(15) (a) Sjöholm, R.; Rairama, R.; Ahonen, M. *J. Chem. Soc., Chem. Commun.* **1994**, 1217−1218. (b) Waldman, H. *Synlett*, **1990**, 627−628.
(16) (a) Fristrup, P.; Le Quement, S.; Tanner, D.; Norrby, P.-O. *Organometallics* **2004**, *23*, 6160−6165. (b) Linde, C.; Koliai, N.; Norrby, P.-O.; Åkermark, B. *Chem. Eur. J.* **2002**, *8*, 2568−2573. (c) Rasmussen, T.; Jensen, J. F.; Østergaard, N.; Tanner, D.; Ziegler, T.; Norrby, P.-O. *Chem. Eur. J.* **2002**, *8*, 177−184.
(17) (a) Yamamoto, Y.; Schmid, M. *J. Chem. Soc., Chem. Commun.* **1989**, 1310−1312. (b) Murakami, M.; Ito, H.; Ito, Y. *J. Org. Chem.* **1993**, *58*, 6766−6770. (c) Barrett, A. G. M.; Seefeld, M. A.; White, A. J. P.; Williams, D. J. *J. Org. Chem.* **1996**, *61*, 2677−2685.

Table 1. One-Pot Procedure for the Synthesis of Amino Alcohols **4a**−**f** (Scheme 3)[a]

entry	imine	X	amino alcohol	isolated yield (%)	anti/syn[b]
1	**3a**	H	**4a**	76	90:10
2	**3b**	OMe	**4b**	70	95:5
3	**3c**	Me	**4c**	82	85:15
4	**3d**	Cl	**4d**	85	95:5
5	**3e**	COOEt[c]	**4e**	73	95:5
6	**3f**	CF_3	**4f**	86	95:5

[a] (i) **2**, Zn, THF; (ii) MeONa, MeOH, 60 °C. [b] From ^{1}H NMR. [c] EtONa in EtOH was used for the deprotection, step (ii).

4). Interestingly enough, benzoyl migration could be suppressed, and the amino ester **5a** was isolated as the sole product in 80% yield. However, the diastereoselectivity was only 1.2:1, in favor of the syn product. Due to the low diastereoselectivity with this substrate, allylations with indium were not pursued further.

To attain a single product, a one-pot procedure was developed to give the deprotected amino alcohol **4** directly. Thus, **3a** was allylated in THF using zinc and **2**, and the reaction mixture was filtered. The crude reaction mixture was then treated with a solution of sodium methoxide in methanol at 60 °C. Subsequent workup and purification by column chromatography yielded compound **4a** in 76% with a diastereomeric ratio of 10:1 in favor of the anti isomer. Imines **3b**−**f** were subjected to the same procedure; the yields and anti/syn ratios are collected in Table 1. The diastereomeric mixtures could not be separated by flash chromatography. However, simple recrystallization in all cases furnished the pure anti amino alcohols **4**.

Hammett Study. In the competition studies, the reactions can be followed by monitoring either appearance of products or, if no significant side reactions are occurring, disappearance of starting material. Since the reaction of each imine yields four initial products (syn and anti isomers of **5** and **6**, respectively), and the isolated yields in the reactions uniformly are high (Table 1), we decided to monitor the concentrations of imines **3** using GC with anthracene as internal standard. We postulate that the reaction order in all reactants is the same for all imines. Furthermore, we assume that the reaction is first order in imine. Under these conditions, the imine concentrations will follow eq 1, where subscript "0" denotes initial concentration, X is the substituted imine **3b**−**f**, H is the unsubstituted imine **3a**, and k_{rel} is the relative reaction rate of the two imines.

$$\ln\left(\frac{X_0}{X}\right) = k_{rel} \ln\left(\frac{H_0}{H}\right) \qquad (1)$$

Thus, by plotting $\ln(X_0/X)$ versus $\ln(H_0/H)$, we obtain the relative reaction rate $k_{rel} = k_X/k_H$ as the slope. We then plot $\log(k_{rel})$ versus σ_X in the standard Hammett plot to obtain the reactivity parameter ρ as the slope and also to check the correlation against different types of σ values.

The five competition experiments between imine **3a** and imines **3b**−**f** were performed in THF at ambient temperature. Initial studies indicated that the allylation, after an initial lag phase, was too rapid to allow a representative sampling. The allylic reagent **2** was therefore added in portions, ensuring that samples could be withdrawn at evenly spaced conversions. We were concerned that in the absence of reagent **2**, the metal might consume the imine in pinacol-type reactions, but a stability test showed that the imine **3a** was stable in the presence of zinc. In addition, the kinetic plots all yielded straight lines with correlation coefficients of $r^2 > 0.99$ (Figure 1). It is unlikely that such straight lines could be obtained if significant amounts of imines participated in side reactions. The relative rates and different σ values for all substrates **3** are shown in Table 2.

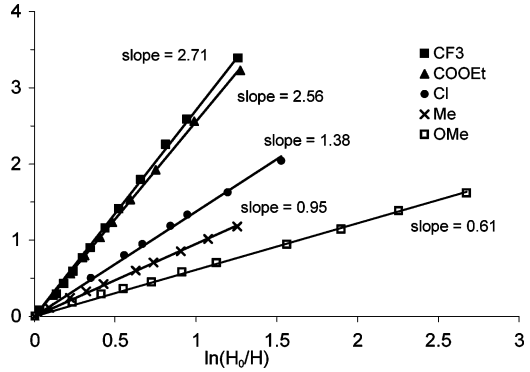

Figure 1. Kinetic data for competitive allylation of imines **3b**−**f**.

Table 2. Rates and σ Values for Imines **3**[a]

substrate	X	σ	σ^+	$\sigma^\bullet$	k_{rel}	$\log(k_{rel})$
3b	OMe	−0.27	−0.78	0.24	0.61	−0.214
3c	Me	−0.17	−0.31	0.11	0.95	−0.022
3d	Cl	0.23	0.11	0.12	1.38	0.138
3e	COOEt	0.45	0.48	0.35[b]	2.56	0.408
3f	CF_3	0.54	0.61	0.08	2.71	0.432

[a] From refs 18 and 19. [b] The $\sigma^\bullet$ value for COOMe was used.

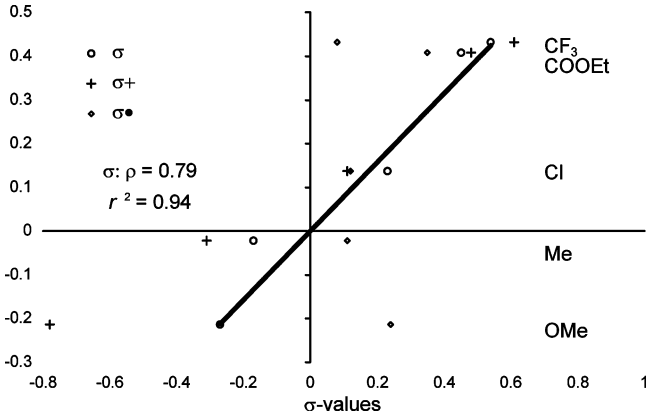

Figure 2. Hammett plot of $\log(k_{rel})$ vs σ, σ^+, and $\sigma^\bullet$ values.

The resulting k_{rel} values are used in the Hammett plots shown in Figure 2. It can be seen that the fit is best using the regular σ values, with a correlation coefficient of $r^2 = 0.94$ and a slope of $\rho = 0.79$. Trying to employ the σ^+ values results in an inferior correlation with $r^2 = 0.67$ (line not shown). One of the main goals of the current Hammett study is to differentiate between closed shell or radical mechanisms, which can be done by comparing the fits to σ and $\sigma^\bullet$ values, respectively. Several different sets of $\sigma^\bullet$ values are available, each with its own advantages. In our case, the conclusions are independent of which set is used, so only the results using the Creary $\sigma^\bullet$ values[19a] are discussed here. It can be clearly seen that the fit to the $\sigma^\bullet$ values is much worse, excluding the possibility of a

(18) Hansch, C.; Leo, A.; Taft, R. W. *Chem. Rev.* **1991**, *91*, 165−195.
(19) (a) Creary, X.; Mehrsheikh-Mohammadi, M. E.; McDonald, S. *J. Org. Chem.* **1987**, *52*, 3254−3263. (b) Dust, J. M.; Arnold, D. R. *J. Am. Chem. Soc.* **1983**, *105*, 1221−1227. (c) Jiang, X.-K.; Ji, G.-Z. *J. Org. Chem.* **1992**, *57*, 6051−6056. (d) Hansch, C.; Gao, H. *Chem. Rev.* **1997**, *97*, 2995−3059.

single-electron transfer (SET) mechanism. In particular the COOEt and CF_3−groups provide an interesting comparison. The two groups have similar σ and σ^+ values, but differ strongly for $\sigma^\bullet$; the ester can stabilize a radical through resonance, whereas the CF_3 group cannot. Thus, the two groups should induce very different rates in a radical reaction, but in the current study, the rates of the two substrates are similar. In addition, none of the groups employed here has a negative $\sigma^\bullet$ value, but still we see that electron-donating substituents retard the reaction.

Going back to the Hammett plot using the regular σ values, the weakly positive ρ is consistent with a nucleophilic attack on the imine and indicates that the electrophilicity of the imine has a higher influence on the rate than the ability of the imine nitrogen to coordinate to the metal.

The Hammett study strongly indicates that the allylic bromide initially reacts with zinc to form an organometallic reagent, which subsequently reacts with the imine. This opens up the possibility to study the reaction computationally with a fair accuracy. The SET mechanism would in principle require high-level methods able to calculate accurate structures and energies for open shell species on a metal surface. Such calculations are possible today, but well beyond our resources. However, with the current data in hand, we estimate that the reaction path can be studied starting from the isolated organometallic reagent. We have previously been involved in several computational studies on the addition of isolated zinc reagents to carbonyl compounds.[20] The goal of the current study is to understand the observed diastereoselectivity in the reaction.

Computational Study. We have initiated the study using small model complexes, first to enable us to select a suitable computational methodology, then to screen all potential paths for the reaction. Subsequently, the most promising reaction paths have been studied using the full substrate **3a**, to give final predicted selectivities. All calculations have been run in Jaguar[21] using the B3LYP functional[22] in combination with the LACVP* basis set.[23] All gas-phase transition states were verified by normal analysis obtained from a mass-weighted force-constant matrix built up with analytical energy second derivatives. Each transition state displayed exactly one mode with a negative eigenvalue, as required. The corresponding eigenmodes were inspected visually in Molekel[24] and found to correspond to Zimmerman−Traxler transition states, as indicated in Figure 3. As a further validation, a sample transition state structure of the small model system was displaced forward and backward along the negative eigenmode and subjected to energy minimization, yielding the expected reactant and product.

We first studied the neutral and cationic forms of the small model system (Figure 3), in the gas phase and in solvent.

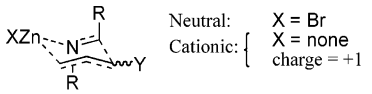

Small model: R = Me, Y = H
Intermediate model: R = Me, Y = OOCH
Large model: R = Ph, Y = OOCH

Figure 3. Model systems employed in the computational study.

Calculations in solvent use the PB-SCRF method[25] in Jaguar, employing parameters suitable for THF (dielectric constant 7.43, probe radius 2.52372 Å). PB-SCRF is a continuum solvation model, where the molecule is put into a reaction field consisting of surface charges on a solvent accessible surface constructed using a hypothetical spherical solvent probe molecule with the indicated radius.[26] The wave function and the reaction field charges are solved iteratively until self-consistency is reached. In our experience, the major role of this electrostatic model is to screen excessive charge separation. For other metal-assisted reactions, we have shown that solvation models of this type give agreement with experimental data in cases where gas-phase calculations deviate strongly.[27] In the current case, we found that for the small model system, the neutral complex (including the bromide counterion) gave very similar results in the gas phase and in solvent. The six-membered rings of the Zimmerman−Traxler transition states were virtually superimposable. Furthermore, the energy difference between the boat and chair forms was found to be the same in the gas phase and in solvent (16 kJ/mol in favor of the chair). The position of the bromide did differ between the two calculations, and the loose coordination of the bromide was found to give severe convergence problems in the solvent calculations. We also tested the cationic model system (without the bromide counterion). Gratifyingly, the structures obtained with the cationic model system in solvent were very close to those obtained with the bromide ion present, and the relative energy of the boat and chair forms only shifted slightly, to 14 kJ/mol. Not unexpectedly, when the cationic system was reconverged in the gas phase, the structures were distorted, even though the relative energy of the boat and the chair was still reasonable, 20 kJ/mol.

From previous projects,[27] we have found that energies calculated with the continuum solvent model gives a fair correspondence with experimental ratios, but for a quantitative agreement we frequently also need to account for the vibrational component of the free energy. With our current resources, this component must be determined from gas-phase calculations, and the combination of this contribution with the solvated energies is only valid if the geometries in the gas phase and solvent are similar. Thus, in the current approach, we have determined all transition states both in solvent and in the gas phase, verified the similarity of the structures by superimposition, and performed a vibrational analysis in the gas phase. The vibrational analysis was used both to verify that the eigenmode corresponding to the single negative eigenvalue indeed corresponds to the

(20) (a) Rasmussen, T.; Norrby, P.-O. *J. Am. Chem. Soc.* **2001**, *123*, 2464−2465. (b) Rudolph, J.; Rasmussen, T.; Bolm, C.; Norrby, P.-O. *Angew. Chem., Int. Ed.* **2003**, *42*, 3002−3005. (c) Rudolph, J.; Bolm, C.; Norrby, P.-O. *J. Am. Chem. Soc.* **2005**, *127*, 1548−1552. (d) Cozzi, P. G.; Rudolph, J.; Bolm, C.; Norrby, P.-O.; Tomasini, C. *J. Org. Chem.* **2005**, *70*, 5733−5736.

(21) *Jaguar 4.2*; Schrödinger, Inc.: Portland, OR, 2000. For the most recent version, see: http://www.schrodinger.com.

(22) (a) Becke, A. D. *J. Chem. Phys.* **1993**, *98*, 5648−5652. (b) Lee, C.; Yang, W.; Parr, R. G. *Phys. Rev. B* **1988**, *37*, 785−789. (c) Stephens, P. J.; Devlin, F. J.; Chabalowski, C. F.; Frisch, M. J. *J. Phys. Chem.* **1994**, *98*, 8, 11623−11627.

(23) LACVP* uses the 6-31G* basis set for all light elements and the Hay-Wadt ECP and basis set for Zn and Br; see: Hay, P. J.; Wadt, W. R. *J. Chem. Phys.* **1985**, *82*, 270−283.

(24) *Molekel*, version 4.3, 2002, Stefan Portmann, CSCS/ETHZ; see http://www.cscs.ch/molekel/.

(25) Marten, B.; Kim, K.; Cortis, C.; Friesner, R. A.; Murphy, R. B.; Ringnalda, M. N.; Sitkoff, D.; Honig, B. *J. Phys. Chem.* **1996**, *100*, 11775−11788.

(26) For an illuminating discussion about implicit solvation models in general, see: Cramer, C. *Essentials of Computational Chemistry: Theories and Models*; Wiley: New York, 2002.

(27) (a) Hagelin, H.; Åkermark, B.; Norrby, P.-O. *Chem. Eur. J.* **1999**, *5*, 902−909. (b) Norrby, P.-O.; Mader, M.; Vitale, M.; Prestat, G.; Poli, G.; *Organometallics* **2003**, *22*, 1849−1855. (c) Kieken, E.; Wiest, O.; Helquist, P.; Cucciolito, M. E.; Flores, G.; Vitagliano, A.; Norrby, P.-O. *Organometallics* **2005**, *24*, 3737−3745.

Table 3. Calculated Relative Transition State Energies for the Intermediate Model System (Figure 3), in kJ/mol

TS conformation	allyl configuration	C═O rel to Zn[a]	gas phase ΔE‡	gas phase ΔΔG‡ [b]	solvent (THF) ΔE‡	product
chair	*Z*	prox	21	5	33	anti
chair	*Z*	dist	2	1	0	anti
chair	*E*	prox	18	0	16	syn
chair	*E*	dist	0	0	0	syn
boat	*Z*	prox	1	6	9	syn
boat	*Z*	dist	27	1	36	syn
boat	*E*	prox	27	1	27	anti
boat	*E*	dist	14	0	13	anti

[a] Of the two possible orientations of the carboxylate−allyl bond, in one the C═O bond will be oriented toward Zn (prox), in the other it will be oriented away (dist). [b] The relative vibrational corrections (including ZPE) at 298 K, add to $\Delta E^{\ddagger}$ to obtain relative free energies.

expected reaction coordinate and to calculate the free energy contribution (at 298 K, including ZPE). The free energy adjustment was then added to the corresponding energy determined in solvent, to arrive at a composite free energy which is our best estimate of the free energy in solvent. For these calculations, it is clear from the initial results that the gas-phase calculations must be performed for the neutral complex. For the calculations run in solvent, the presence of the counterion did not seem to have an influence on the quality of the results, since both the structure and energy were insensitive to the presence of the bromide. We therefore elected to perform the solvated calculations using the cationic model system, since the presence of the loosely coordinated bromide ion had a severe detrimental effect on the convergence properties of the transition state optimizations.

Moving on to the intermediate model system, we have investigated the possible variations in the Zimmerman−Traxler transition state shown in Figure 3. Thus, the addition can proceed via a boat or a chair transition state, the position of the carboxylate in the allylic reagent can be either *E* or *Z*, and finally, the carboxylate moiety can rotate around the bond to the allyl moiety, pointing the carbonyl either toward or away from the Zn atom. Coordinate scanning indicated that only these two orientations are feasible for the carboxylate moiety. The energies for the eight possible transition states of the intermediate model are shown in Table 3.

We first note that the vibrational contributions, although large in absolute value (see the Supporting Information), contribute very little to the *relative* energy of the transition states. The only significant effect is for the transition states with *Z*-configuration where the C═O bond is oriented toward Zn, limiting the vibrational freedom and therefore incurring a slight energy cost, ca. 5 kJ/mol. In the boat, the carbonyl oxygen actually coordinates to Zn (distance Zn−O = 2.16−2.17 Å). In the gas phase, the prox-*Z*-boat is therefore one of the best conformations and the only boat with any significance. However, it is clear that this coordination is less favorable in solvent, where only dist-chair conformations have a low enough energy to contribute a significant amount of product. These two are isoenergetic, whereas the experimentally observed ratios (Table 2) correspond to an activation free energy difference of 6−8 kJ/mol.

The above results were somewhat encouraging, but not sufficiently accurate to be useful, so we decided to increase the size of the model system. The solvent data for the 8 TS isomers of the large model system, which includes the two phenyl groups of substrate **3a**, are shown in Table 4.

Table 4. Calculated Relative TS Energies in Solvent for the Large Model System (Figure 3), in kJ/mol

TS conformation	allyl configuration	C═O rel to Zn[a]	solvent (THF) ΔE‡	product
chair	*Z*	prox	14	anti
chair	*Z*	dist	0	anti
chair	*E*	prox	18	syn
chair	*E*	dist	10	syn
boat	*Z*	prox	3	syn
boat	*Z*	dist	33	syn
boat	*E*	prox	35	anti
boat	*E*	dist	25	anti

[a] Of the two possible orientations of the carboxylate−allyl bond, in one the C═O bond will be oriented toward Zn (prox), in the other it will be oriented away (dist).

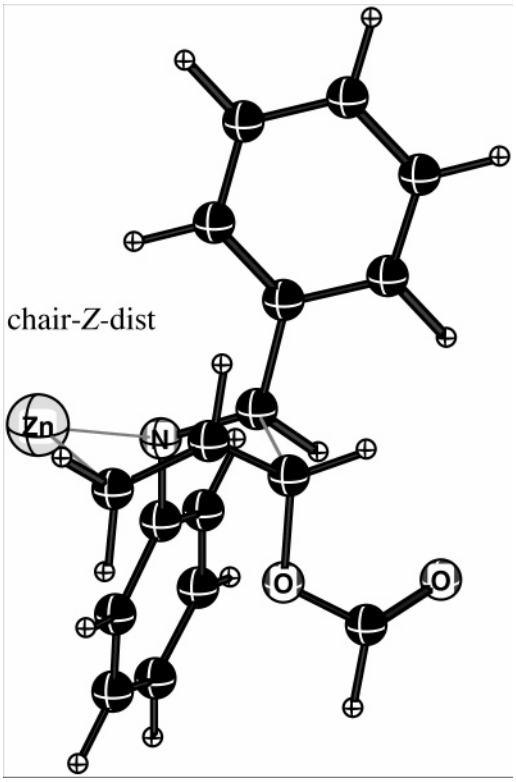

Figure 4. Best transition state with the large model system, the chair-*Z*-dist isomer, leading to the anti product.

The data in Table 4 indicate that only three transition states are of interest. The lowest energy TS is the chair-*Z*-dist isomer (Figure 4), leading to the anti diastereomer, which is also observed as the major product. Two low energy transition states lead to the syn products, boat-*Z*-prox and chair-*E*-dist (Figure 5). We know from the vibrational analysis using the intermediate model system that the vibrational contribution is significant for the boat-*Z*-prox TS. Thus, for the three lowest energy structures, we also located the transition states for the large model system using the neutral gas-phase structures (including the bromide counterion). After verifying the structural similarity with the corresponding solvated structures, we performed a vibrational analysis to arrive at the final composite free energies described earlier. In this final analysis, the chair-*Z*-dist isomer is still the global optimum, but now the boat-*Z*-prox is 8 kJ/mol higher, and the isomer is shifted to 12 kJ/mol. These numbers are in very good agreement with the experimental syn/anti difference

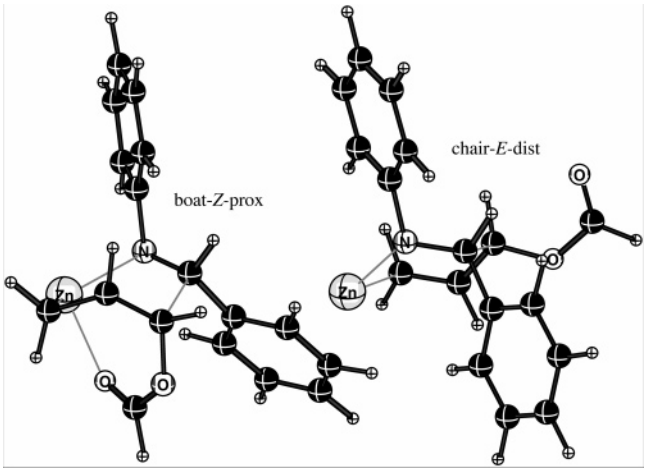

Figure 5. Two best transition states leading to the minor syn products, the boat-*Z*-prox and chair-*E*-dist isomers.

of ca. 8 kJ/mol and indicates that the minor syn-isomer predominately arises from boat-*Z*-prox TS.

Finally, we want to note that a comparison of all potential transition states is equivalent to implicitely postulating that the system is under Curtin−Hammett conditions,[28] that is, that equilibration of all possible forms of the organometallic allyl reagent is fast compared to reaction with the imine. This point has not been investigated computationally, but it has been observed experimentally that the diastereomeric ratio of the product is insensitive to the *E*/*Z* ratio in the allylic reagent.[11c] Since none of the paths from the *E*-reagent to the anti product have a low energy (Table 4), we regard the Curtin−Hammett assumption as validated.

(28) Maskill, H. *The Physical Basis of Organic Compounds*; Oxford University Press: Oxford, 1985; pp 293−295.

Conclusions

A new zinc-mediated addition reaction has been developed for the synthesis of amino alcohols from imines and benzoyloxyallyl bromide. A combined Hammett and computational study indicates that the addition takes place in homogeneous phase between an initially formed organometallic allyl reagent and the imine in a Zimmerman−Traxler transition state. The main reactivity-determining factor in the addition is the electrophilicity of the imine carbon, not the ability of the imine nitrogen to coordinate to the metal. There is very good agreement between the computed and observed selectivity in the reaction.

Acknowledgment. The Lundbeck Foundation is gratefully acknowledged for financial support.

Supporting Information Available: Experimental procedures and characterization of compounds; data from kinetic runs; Cartesian coordinates and energies for all calculated structures. This material is available free of charge via the Internet at http://pubs.acs.org.

JA054706A